# Distribution of Photosensitizers in Bladder Cancer Spheroids: Implications for Intravesical Instillation of Photosensitizers for Photodynamic Therapy of Bladder Cancer

Zhengwen Xiao[1], Christian B. Hansen[2, 3], Theresa M. Allen[2], Gerald G. Miller[4] and Ronald B. Moore[1]

Departments of [1]Surgery, [1]Oncology, and [2]Pharmacology, University of Alberta, Edmonton, Alberta, Canada
[3]AltaRex Corporation, Edmonton, Alberta, Canada.
[4]Noujaim Institute for Pharmaceutical Oncology Research, Faculty of Pharmacy & Pharmaceutical Sciences, University of Alberta, Edmonton, Alberta, Canada

*Received March 1, 2005; Revised September 7, 2005; Accepted September 19, 2005; Published September 28, 2005*

**ABSTRACT PURPOSE**: Uniform intratumor distribution of sufficient photosensitizer is one of the important aspects of photodynamic therapy for solid tumors. **METHODS**: Multicellular spheroids derived from a human transitional cell carcinoma cell line (MGHU3) were used as a surrogate system of tiny solid tumors to study intratumor distribution of photosensitizers. Photosensitizers included Photofrin, hypocrellins (HBEA-R1/R2, HBBA-R2), aluminum phthalocyanine chloride (AlPC), benzoporphyrin derivative monoacid ring A (BPD-MA), protoporphyrin-IX (PpIX), and liposomal formulations of HBBA-R2 and BPD-MA. Spheroids were incubated with various doses of the above drugs for 1–4 hours, and were examined by confocal microscopy. **RESULTS**: Histology showed all cells were healthy in spheroids less than 400 μm in diameter. Scanning electron microscopy showed tight cell-to-cell interdigitation in spheroids. HBEA-R1/R2 distributed more uniformly in spheroids than other drugs. Free hypocrellins and BPD-MA penetrated spheroids centripetally deeper than AlPC, Photofrin, and PpIX. Liposomal HBBA-R2 and BPD-MA penetrated less than their free formulations. **CONCLUSIONS**: The spheroids mimic solid tumors prior to neovascularization. Based on drug distribution in spheroids, hypocrellins and BPD-MA appear superior to Photofrin, AlPC and PpIX for intravesical administration for bladder cancer phototherapy.

**Corresponding Author:** Ronald B. Moore, Department of Surgery, University of Alberta, 2D2 Walter Mackenzie Health Sciences Centre, 8440-112 Street, Edmonton, Alberta, Canada T6G 2B7. rmoore@cha.ab.ca

**Abbreviations:**
AlPC, Aluminum phthalocyanine chloride; AUC, area under the intensity *vs.* spheroid diameter curve; BPD-MA, Benzoporphyrin derivative monoacid ring A; CLSM, confocal laser scanning microscope; D-MEM, Dulbecco's modified Eagle's medium; DMSO, dimethyl sulfoxide; DPPC, dipalmitoyphosphatidylcholine; HB, hypocrellin B; HBBA-R2, n-butylaminated HB; HBEA-R1/R2, ethanolaminated HB; PBS, phosphate-buffered saline; PDT, photodynamic therapy; PEG2000-DSPE, polyethylene glycol ($M_r$ 2000)-distearoylphosphatidylethanolamine; PF, Photofrin or porfimer sodium; PpIX, Protoporphyrin IX; SEM, scanning electron microscopy; SL, sterically stabilized (Stealth) liposome.

## INTRODUCTION

In photodynamic therapy (PDT) of cancers, a photosensitizer, light, and oxygen are photochemically interactive to cause cell death (1). Several mechanisms have been proposed for PDT mediated tumor destruction, including direct and indirect cell killing (2,3). Direct cell killing depends on selective accumulation of sufficient amounts of a photosensitizer in tumor (3). The uptake, distribution and retention of a sensitizer in tumor are dependent on the route and mode of delivery, as well as the physicochemical properties (*e.*g. lipophilicity) of the drug. For instance, lipophilic photosensitizers need to be incorporated into delivery vehicles for *in vivo* administration, and they are taken up by neoplastic cells partially *via* a receptor-mediated pathway, and binding mainly with cellular membranes (4,5). *In situ* photoactivation of these drugs may therefore result in direct cell killing (6,7). In contrast, hydrophilic sensitizers, such as tri- and tetrasulfonated porphyrins and phthalocyanines, can be administered as free drugs. They bind in a noncovalent fashion to plasma proteins (albumin and globulins) and subsequently localize in vascular stroma of normal and tumor tissues (8,9). Photoactivation of these drugs causes damage to the microvasculature, leading to vascular stasis and tumor infarction (indirect cell killing) (10).

Damage to the microvasculature is a prominent *in vivo* tumor response to PDT with Photofrin (porfimer sodium), the most widely used photosensitizer (1, 2). Patients treated with Photofrin-based PDT, however, exhibit prolonged skin phototoxicity (11). This side effect is attributable to prolonged retention of the photosensitizer in the skin. In addition, following systemic administration, Photofrin-based PDT causes bladder shrinkage in patients with bladder cancers

(12). These side effects have prompted the search for new photosensitizers and new routes of drug administration. Phthalocyanines, benzoporphyrin derivatives, and hypocrellins are second-generation photosensitizers that can be activated by longer wavelengths (> 630 nm) than Photofrin. Furthermore, the monomeric properties of these second-generation photosensitizers promote more rapid clearance from normal tissues; therefore prolonged skin phototoxicity may not be problematic (13,14,15).

Topical administration of liposomal formulations of photosensitizers not only broadens the application of potent monomeric, lipophilic photosensitizers, but also facilitates uptake by tumor cells due to direct contact of the liposomal drug with tumor, thereby reducing distribution to the reticuloendothelial system (5,16). To a great extent, the efficacy of PDT for bladder cancer depends on the degree of intratumor uptake of photosensitizers and their phototoxicity to cancer cells. Selection of appropriate photosensitizing drugs for whole bladder PDT therefore requires knowledge of dose- and time-dependent accumulation of the drugs in tumor, as well as their phototoxicity. Multicellular spheroids have been used as surrogates of tiny tumors for studying distribution and efficacy of chemo- and radio-therapeutic agents (17,18,19). In this study, the distribution and retention of several second-generation photosensitizers, as well as their liposomal formulations, in human bladder cancer cell spheroids were investigated. The results were compared with those of Photofrin, to explore the potential of these new photosensitizers for PDT of superficial bladder cancers following intravesical administration.

## MATERIALS AND METHODS

*Tumor cells and spheroid growth kinetics*. The spheroids were cultured from a moderately differentiated human transitional cell carcinoma cell line (MGHU3). MGHU3 cells were generously provided by Dr. Y. Fradet at the University of Laval, Quebec. Spheroids were generated by adding $2 \times 10^6$ cells to 60 mL of Dulbecco's modified Eagle's medium [D-MEM (Gibco/BRL, Burlington, ON)], supplemented with 10% fetal calf serum and antibiotics. The spheroids grew in spinner flasks on a stir-plate under standard cell culture conditions (37°C, 5% $CO_2$). Half of the medium was replaced with fresh medium 4 days later and every other day thereafter. To establish the growth kinetics of the spheroids, samples were taken every two days. The spheroids' size was measured by microscopy. Spheroids reaching 300 μm in diameter (at 8 – 10 days) were processed for histology to determine if there were necrotic cells in the center, or for scanning electron microscopy (SEM) to study cell-cell connections on the spheroid surface and in its cross section.

*Photosensitizers*. (1) Photofrin was provided by QLT Inc. (Vancouver, BC). It was dissolved in 5% dextrose (Abbott Laboratories, Montreal, QC), then diluted with serum-free medium immediately before incubation with spheroids. (2) Hypocrellin B (HB, Altarex Corp. Edmonton, AB) included HBEA-R1/R2 (ethanolaminated HB, $M_r$ 614), HBBA-R2 (n-butylaminated HB, $M_r$ 636), and liposomal HBBA-R2. We have previously reported the physical and chemical properties of hypocrellins in detail (15). Free hypocrellins were first dissolved in ethanol, and then diluted with serum-free medium. The liposomal preparations will be discussed below. (3) Benzoporphyrin derivative monoacid ring A (BPD-MA, $M_r$ 718) and liposomal BPD-MA were provided by QLT Inc. BPD-MA was dissolved in dimethyl-sulfoxide (DMSO) and then diluted with serum-free medium prior to use. Liposomal BPD-MA (2.0 mg/ml stock solution) was further diluted with serum-free medium immediately before use. (4) Aluminum phthalocyanine chloride (AlPC) was purchased from Acros Organics ($M_r$ 575), and (5) protoporphyrin IX (PpIX, $M_r$ 562.7) was purchased from Sigma Chemical Co. (St. Louis, MO). AlPC and PpIX were first dissolved in DMSO and then diluted with serum-free medium.

*Liposomal hypocrellin formulation.* The procedures of liposome preparation were described previously (20). Dipalmitoyphosphatidylcholine (DPPC) was purchased from Avanti Polar Lipids, and maleimide-PEG2000-distearoylphosphatidylethanolamine (DSPE) was purchased from Shearwater Polymers Inc. (Huntsville, AL). Long circulating, sterically stabilized liposome (SL) formulation of HBBA-R2 was composed of DPPC/maleimide-PEG2000-DSPE (94:6 molar ratio). HBBA-R2 was loaded into pre-formed SL at a 15:1 lipid to drug molar ratio. Liposomes were prepared by hydrating a dried thin film of lipids to a final concentration of 10 m*M* lipid with 20 m*M* HEPES 140 m*M* NaCl, pH 7.4. HBBA-R2 dissolved in solvent (20 m*M* in methanol) was heated to 65°C and injected dropwise, into a 65°C solution of liposomes. The resulting hypocrellin-

liposomes were extruded through 100 nm and 80 nm polycarbonate membranes using a Lipex® Biomembranes extruder (Vancouver, BC) to give an average vesicle size of 100 nm. The liposomes were then purified by gel filtration and assayed for lipid and drug concentrations. A final lipid to drug molar ratio of 20:1 was typically obtained. Liposomal HBBA-R2 was further diluted with serum-free medium before use.

*Photosensitizer distribution in spheroids*. Spheroids 200- to 400-μm in diameter were incubated with Photofrin up to 15 μg/ml or graded doses (0 – 20 μ*M*) of other photosensitizers and liposomal drugs for different time-points (1 – 4 h). Plain liposomes (~300 μ*M* lipids) were also incubated with spheroids for lipid-only controls. More than 5 spheroids were incubated in a 35-mm suspension culture dish (Corning, NY) in 2 ml of solution containing various drugs at 37°C. At the end of the incubation, the spheroids were gently washed with phosphate-buffered saline (PBS) three times, and imaged using a confocal laser-scanning microscope (CLSM). The CLSM system (Molecular Dynamics, CA) consisted of an argon-krypton laser, a Nikon inverted microscope, and ImageSpace® software (version 3.2, Molecular Dynamics, CA) to analyze the images (analyzing intensity profile, 3–dimension reconstruction). Confocal parameters are listed as follows: 20×/0.55 objective lens; 488/568 nm exciting wavelengths (for AlPC, 647 nm was used); 488/568 nm beam-splitter (for AlPC, 647 nm beam-splitter was used); 590 nm long-pass (LP590) barrier filter for fluorescence detection (for AlPC, a LP660 filter was used). The interval between optical slices was 2 – 3 μm. Five typical spheroids from each time-point and drug concentration were scanned from the surface (top) to the center, and the images were stored for further analysis.

Fluorescence intensity histograms in the central sections of each spheroid were created using ImageSpace® software. From these histograms, areas under the intensity *vs*. spheroid diameter curve (AUC) were calculated with the trapezoid area formula (21), and normalized by each spheroid's diameter. These averaged AUCs represent drug accumulation in spheroids.

## RESULTS

*Growth characteristics of MGHU3 spheroids*

The spheroids' growth kinetics is shown in Figure 1.

At 8 – 10 days, the average diameter of the spheroids was around 300 μm. The spheroids continue to grow to 600 – 700 μm at 4 weeks, and attach to each other thereafter (Figure 1). Histological examination showed all the cells from the periphery to the center were healthy in spheroids less than 400 μm in diameter.

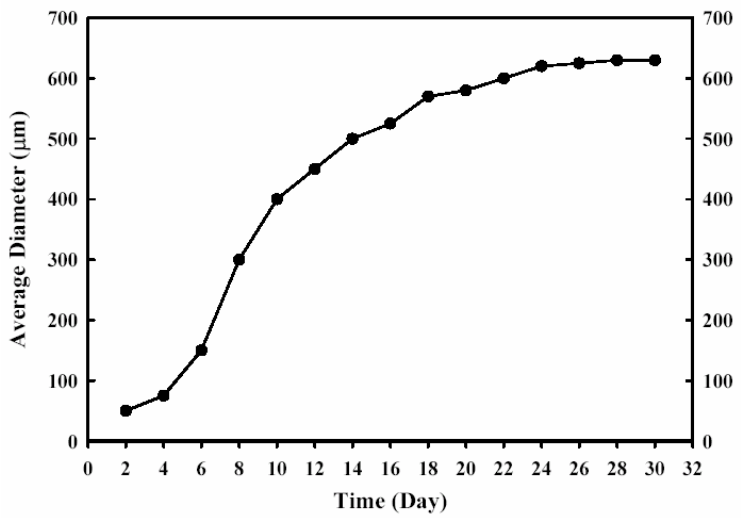


**Figure 1.** Growth kinetics of MGHU3 spheroids cultured in spinner flasks.

In those spheroids greater than 500 μm, a central zone of degenerative changes (hypoxia or necrosis) was observed (data not shown). Scanning electron microscopy showed a network-like extracellular matrix covering the spheroid, and tight cell-cell interdigitation of microvilli in the cross section (Figs 2, 3).

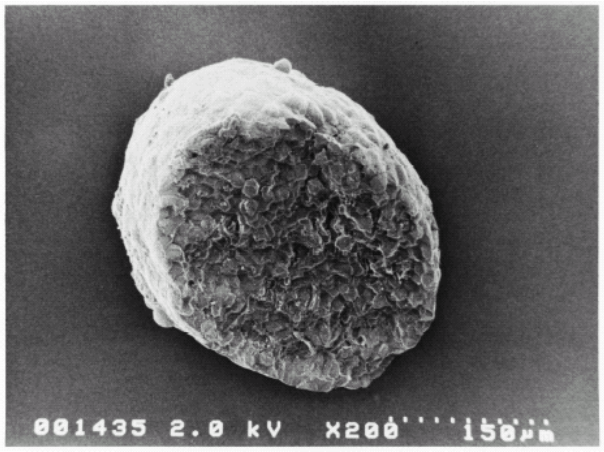


**Figure 2.** SEM microphotograph of a MGHU3 spheroid showing an extracellular matrix network covering the surface, which models a small tumor prior to neovascularization.

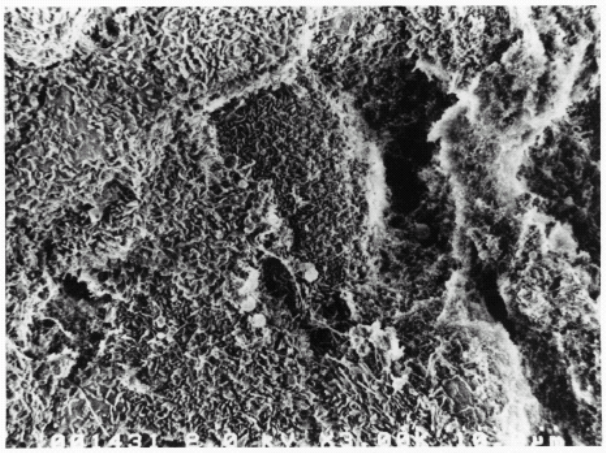

**Figure 3.** SEM microphotograph of a cross section of a spheroid-displaying tumor cells in tight contact with interdigitation of microvilli.

*Intraspheroid distribution of photosensitizers*

Figure 4 shows a series of confocal sections scanned from the top surface to the center of a spheroid incubated with HBEA-R1/R2. HBEA-R1/R2 was distributed from the surface to the center of a spheroid with fluorescence intensity in the peripheral sections slightly higher than in the central sections.

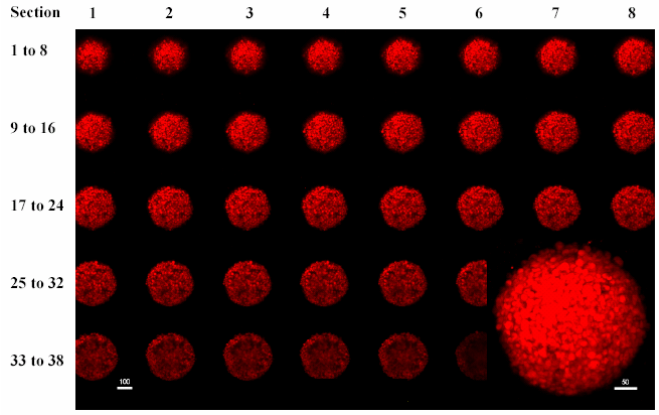


**Figure 4.** Serial confocal sections from the top surface to the center of a MGHU3 spheroid incubated with 10 μ*M* HBEA-R1 for 2 hours. Inset, a 3-dimension projection of the spheroid showing the spheroid surface. (Bars denote μms).

Penetration and distribution of other photosensitizers in the central sections of spheroids are displayed in Figures 5A–H, and a representative fluorescence intensity histogram across a central section is shown in Figure 5C.

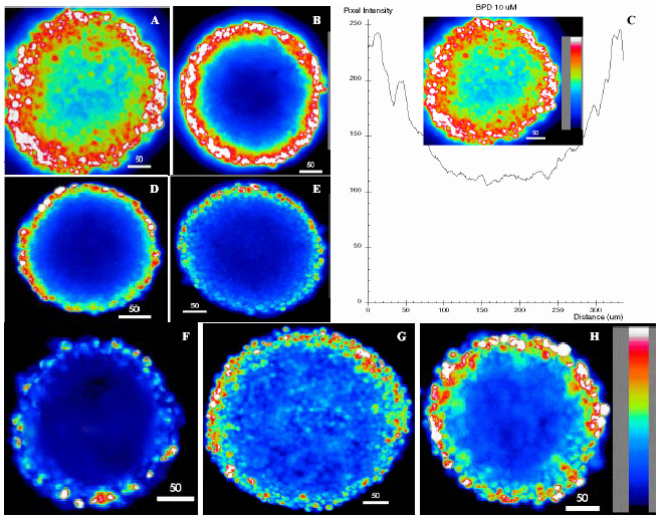


**Figure 5.** Pseudo-color confocal images showing penetration, distribution and intensity profile in the central sections of spheroids incubated with photosensitizers at 37ºC for 4 hours. (A), BPD-MA 10 μ*M* (7.18 μg/ml); (B), liposomal BPD-MA 10 μ*M*; (C), histogram profile of A; (D), AlPC 10 μ*M* (5.75 μg/ml); (E), Photofrin 15 μg/ml; (F), PpIX 10 μ*M* (5.6 μg/ml); (G), HBBA-R2 10 μ*M* (6.36 μg/ml); (H), SL-HBBA-R2 10 μ*M*. (Bars denote μms).

Generally, in these color-coded confocal micrographs, the highest intensity (white) was observed at the spheroid periphery ranging from one to ten cells in depth, and spheroid centers showed the lowest intensity (black-purple). Interestingly, BPD-MA (Fig. 5A) and HBBA-R2 (Fig. 5G) penetrated deeper than AlPC (Fig. 5D), Photofrin (Fig. 5E) and PpIX (Fig. 5F), so that the intensity level of BPD at the center of a spheroid reached almost half of that at the periphery (Fig. 5C). For the latter three drugs, fluorescence was detected only at the spheroid rim (< 3 cellular layers), while at the center virtually no fluorescence was observed (Fig. 5D, 5E, and 5F). For comparison, spheroids incubated with liposomal BPD-MA (Fig. 5B) and liposomal HBBA-R2 (Fig. 5H) also showed high levels of fluorescence at the periphery. However, the intensity levels at the center were lower than that of their free drugs (Fig. 5B *vs*. 5A, and Fig. 5H *vs*. 5G).

To further analyze the fluorescence distribution quantitatively, the average normalized AUC's of various drugs are summarized in Table 1. These AUC's are indications of drug accumulation in spheroids for a given drug to examine the time and dose effects. These AUCs data clearly suggested that spheroids efficiently took up and accumulated BPD-MA, liposomal BPD-MA, hypocrellins and liposomal HBBA-R2.

**Table 1**. Summary of average normalized areas under the intensity *vs*. spheroid diameter curve (AUC) that is an indication of drug accumulation in spheroids. Spheroids were incubated with graded doses of photosensitizers for up to 4 h and scanned by confocal laser scanning microscopy. The intensity profile in a spheroid central section was taken to calculate the AUC and corrected by that spheroid's diameter. Each value was derived from the mean of 5 spheroids.

| Time (h) | PF [a] (5 μg) | PF (10 μg) | PF (15 μg) | PpIX (10 μ*M*) | PpIX (20 μ*M*) | AlPC (5 μ*M*) | AlPC (10 μ*M*) | AlPC (20 μ*M*) |
|---|---|---|---|---|---|---|---|---|
| 1 | ND | ND | ND | ND | ND | ND | 10.74 | 11.84 |
| 2 | 1.84 | 6.92 | 7.73 | 4.75 | 3.38 | 21.76 | 25.84 | 33.38 |
| 4 | 8.21 | 8.75 | 14.42 | 7.71 | 11.19 | 23.76 | 34.55 | 35.76 |

| Time (h) | HBEA (5 μ*M*) | HBEA (10 μ*M*) | HBEA (20 μ*M*) | HBBA (5 μ*M*) | HBBA (10 μ*M*) | HBBA (20 μ*M*) | BPD-MA (5 μ*M*) | BPD-MA (10 μ*M*) |
|---|---|---|---|---|---|---|---|---|
| 1 | 6.44 | 12.48 | 15.70 | ND | ND | ND | ND | ND |
| 2 | 22.24 | 41.16 | 54.23 | 20.31 | 50.94 | 76.27 | ND | ND |
| 4 | 12.71 | 29.65 | 42.82 | ND | 76.17 | 101.8 | 91.54 | 148.0 |

| Time (h) | L-BPD-MA [b] (5 μ*M*) | L-BPD-MA (10 μ*M*) | L-HBBA[c] (5 μ*M*) | L-HBBA (10 μ*M*) | Control (300 μ*M* lipids) |
|---|---|---|---|---|---|
| 2 | ND | ND | 41.45 | 60.69 | ND |
| 4 | 85.73 | 121.29 | 66.98 | 77.24 | 0.53 |

*ND, no data; [a], Photofrin; [b], liposomal BPD-MA; [c], liposomal HBBA-R2.*

The drug accumulation was both time- and dose-dependent, except HBEA-R1/R2, for which the AUC's at 2 h already reached the plateau state. Based on a molar concentration (10 μ*M* incubated for 4 h), the AUC of BPD-MA was close to that of liposomal BPD-MA; two times of that of HBBA-R2 and liposomal HBBA-R2; more than four times of that of AlPC; ten times of that of Photofrin (15 μg/ml) and 18 times of that of PpIX.

## DISCUSSION

Whole bladder PDT has been proven as an effective treatment modality for refractory superficial bladder cancer (12). In whole bladder PDT, sufficient accumulation of the photosensitizer in tumor tissue, compared to underlying normal tissues, is very important to ablate the tumor while maintaining normal bladder function. The main objective of intravesical instillation of photosensitizers is to increase the local tissue (*i.e.* tumor) concentration and decrease systemic uptake of the drug, and thus reduce the undesired side effects (bladder contracture and prolonged photosensitivity). As there is limited data available on the distribution of photosensitizers in tumors after intravesical administration, we carried out the study in order to determine the distribution pattern of both first and second-generation photosensitizers in MGHU3 spheroids. These spheroids resemble small residual bladder tumors prior to vascularization. This study provides a first step for screening photosensitizers with potential intravesical application.

Many factors can effect photosensitizer distribution in cells and tumor. For photosensitizer per se, the structure determines its biological parameters, such as lipophilicity. According to structures, Boyle and Dolphin classified photosensitizers into three major groups (22): (1) Hydrophobic sensitizers are defined as those bearing no charged substituents and which have negligible solubility in water or alcohol. (2) Hydrophilic sensitizers have three or more charged substituents and are freely soluble in water at physiological pH. (3) Amphiphilic sensitizers have two or less charged substituents and are soluble in alcohol or water at physiological pH. Therefore, AlPC falls into the hydrophobic group. PpIX, BPD-MA, and HBBA-R2 are on the borderline between the hydrophobic and amphiphilic groups. HBEA-R1 is amphiphilic. Photofrin is on the borderline between amphiphilic and hydrophilic. The photosensitizers tested in this report included those promising second-generation drugs, as well as the first-generation sensitizer, Photofrin. Hypocrellin B derivatives (HBEA-R1, HBBA-R2) have been documented as potent photosensitizers *in vitro* (15) and *in vivo* (23, 24). However, the more lipophilic HBBA-R2, like BPD-MA (14) and AlPC (13), is not suitable for *in vivo* administration without being incorporated into liposomes or other suitable carriers (5). Photofrin is a mixture of oligo-porphyrins. PpIX was selected

because it is an endogenous sensitizer derived from 5-aminolevulinic acid, which has been used in pre-clinical and clinical trials (25, 26, 27). In general, a concentration-dependent, diffusion driven penetration and accumulation have been demonstrated for each compound tested (Table 1, Fig. 5). In confocal microscopy, the fluorescence levels at spheroid rim are always higher than that in spheroid center (Fig. 5). HBEA-R1 penetrates deeper and distributes more uniformly into spheroids than its analog, HBBA-R2 (Fig. 4), probably because the latter is more lipophilic. HBBA-R2 may have higher affinity for membranous structures, which retards its penetration into the spheroid center. Similar result of decreased penetration of hypericin with increased lipophilicity has been reported (28). Furthermore, the network of hydrophilic extracellular matrix on the spheroid surface may also impede the penetration of lipophilic compounds (29). This extracellular matrix network consists of proteoglycans and glycosaminoglycans, and is not expressed in monolayer cells (28, 29). Photofrin can only penetrate about three cell layers, which may be attributed to its large oligo-porphyrin structures (30). Although BPD-MA has larger molecular size than AlPC and PpIX, it penetrates better than the later two (Fig. 5). Thus, molecular size and lipophilicity are just two of the many factors affecting penetration. Other factors also include drug concentration and availability (aggregation), incubation time, cell cycle, spheroid (or tumor) structures, and drug carriers used. One could speculate that each drug might have a unique distribution pattern, particularly in the diverse clinical settings.

The liposomal formulations of BPD-MA and HBBA-R2 used in this study do not have a drug-targeting role, and provide merely carriers whereby BPD-MA and HBBA-R2 can be administered in monomeric forms. Aggregation can reduce a photosensitizer's bioavailability *in vivo*, and undermine its capacity to interact with light and therefore its effectiveness (31). Compared to free drug, both liposomal BPD-MA and HBBA-R2 have poor penetration into the spheroids, whereas the fluorescence accumulation at the spheroid rim is high (Fig. 5). However, the normalized drug accumulation is similar for both free and liposomal formulations (Table 1). This could be explained in that liposomes may transiently keep the photosensitizers from penetrating due to their size, and the photosensitizers may be taken up as liposome-drug packages by cells in the spheroid rim. Apart from as carriers, liposomes conjugated with monoclonal antibody directed against tumor cells might be exploited for site-specific immunophotodynamic therapy of bladder cancer (32).

Multicellular spheroid provides a good 3-dimensional model for drug distribution studies. Ideally, spheroids should be used to test phototoxicity in an environment mimicking small tumors. However, in our practice, we found that it was difficult to accurately assess the results by using spheroid for phototoxicity study, especially for comparing different kinds of photosensitizers. These limitations include: (a) when spheroids reach sizes of 400 μm or greater, the cells in the center are resistant to photodynamic therapy (PDT) due to hypoxia (33). Phototoxicity is a reciprocal effect of light, drug and oxygen. Since there is no vasculature inside the spheroids to provide tissue oxygen, PDT can easily deplete oxygen and have virtually no effect on cells in the spheroid center (33). The proportion of hypoxic cells is dependent on the spheroid size. The larger the spheroid, the more hypoxic cells versus oxygenated cells. Therefore, to compare phototoxicity among different photosensitizers, spheroid sizes selected should be the same. Practically, it is very difficult, if not impossible. (b) The cells in the spheroid rim accumulated much higher levels of photosensitizers than the cells in the center did (demonstrated in this study). Trypsinization of the spheroids after PDT destroys the 3-D configuration of the spheroids, and mixes up the cells from the rim with the cells from the center. Subsequently sampling of the cells for clonogenic experiments may either overestimate the phototoxicity (by sampling more cells from the rim) or underestimate the phototoxicity of the drug (by sampling more cells from the center of the spheroid). Using monolayer cells to preliminarily screen potent photosensitizers has some advantages, because the three major factors in PDT (drug dose, light dose and oxygen) can be strictly controlled. *In vivo* studies comparing tissue distribution of liposomal hypocrellin *vs.* hypocrellin dissolved in DMSO/saline demonstrated that liposomal hypocrellin reached higher drug levels in tumor, but took a longer time to reach the maximal level than the free drug (34). Similarly, the present study also shows comparable drug accumulation in spheroids between liposomal and free BPD-MA and HBBA-R2 if the incubation time is longer than 2 hours.

In conclusion, the multicellular MGHU3 spheroids resemble small tumors prior to neovascularization, so that drug distribution in spheroids may mimic the situation in residual

bladder tumor. Based on drug distribution in the spheroids *in vitro*, BPD-MA and hypocrellin B derivatives seem to be the most promising candidates for intravesical administration for PDT of bladder cancer. Liposomes can be used as carriers to deliver these potent lipophilic photosensitizers *in vivo*. The liposomal formulations of HBBA-R2 and BPD-MA may be utilized for immunophotodynamic therapy of bladder cancer, given an appropriate targeting antibody.

## ACKNOWLEDGMENTS

Funding support from the Alberta Cancer Board, the Edmonton Civic Employees' Charitable Fund, and the Alberta Heritage Foundation for Medical Research is gratefully acknowledged. Special thanks are to Mr. Bhatnagar for the excellent assistance with confocal microscopy.

## REFERENCES

1. Henderson B W and Dougtherty T J. How does photodynamic therapy work? *Photochem. Photobiol*., **55**: 145-157, 1992.
2. Doughery T J, Gomer C J, Henderson B W, et al. Photodynamic therapy. *J Natl. Cancer Inst.*, **90**: 889-905, 1998.
3. Van Hillegersberg R, Will JK and Wilson JHP. Current status of photodynamic therapy in oncology (review). *Drugs*. **48** (4): 510-527, 1994.
4. Love WG, Duk S, Biolo R, Jori G and Taylor PW. Liposome-mediated delivery of photosensitizers: localization of Zinc (II)-Phthalocyanine within implanted tumors after intravenous administration. *Photochem. Photobiol*., **63**: 656-661, 1996.
5. Reddi E. Role of delivery vehicle for photosensitizers in the photodynamic therapy of tumors (review). *J. Photochem. Photobiol. B: Biol*. **37**: 189-195, 1997.
6. Peng Q, Moan J, Farrants G, Danielsen HE and Rimington C. Localization of potent photosensitizers in human tumor LOX by means of laser scanning microscopy. *Cancer Lett*., **53**: 129-139, 1990.
7. Cuomo V, Jori G, Rihter B, Kenney ME and Rodgers MAJ. Liposome-delivered Si(IV)-naphthalocyanine as a photodynamic sensitizer for experimental tumors: pharmacokinetic and physiotherapeutic studies. *Br. J. Cancer*. **62**: 966-970, 1990.
8. Kessel D, Thompson P, Saatio K and Nantwi KD. Tumor localization and photosensitization by sulfonated derivatives of tetraphenyporphine. *Photochem. Photobiol*., **45**: 787-790, 1987.
9. Jori G and Reddi E. Strategies for tumor targeting by photodynamic sensitizers. In *Photodynamic Therapy of Neoplastic Disease* (Edited by D. Kessel), pp. 117-130. CRC Press, Boca Raton, FL. 1990.
10. Henderson BW, Waldow SM, Mang TS, Potter WR, Malone PB and Dougherty TJ. Tumor destruction and kinetics of tumor cell death in two experimental mouse tumors following photodynamic therapy. *Cancer Res*., **45**: 572-576, 1985.
11. Dougherty TJ, Cooper MT and Mang TS. Cutaneous phototoxic occurrences in patients receiving Photofrin. *Lasers Surg. Med*., **10**: 485-488, 1990.
12. Nseyo UO, Shumaker B, Klein EA and Sutherland K. for the bladder Photofrin study group. Photodynamic therapy using porfimer sodium as an alternative to cystectomy in patients with refractory transitional cell carcinoma in situ of the bladder. *J. Urol*. **160**, 39-44, 1998.
13. Ben-Hut E and Rosenthal I. The phthalocyanines: a new class of mammalian cell photosensitizers with a potential for cancer phototherapy. *Int. J. Radiat. Biol*., **47**: 145-147, 1995.
14. Sternberg E and Dolphin D. An overview of second generation drugs for photodynamic therapy including BPD-MA. In Spinelli P, Dal Fante M, Marchesini R, eds. Photodynamic Therapy and Medical Lasers. *Excerpta Medica* 470-474, 1993.
15. Estey EP, Brown K, Diwu Z, Liu J, Lown JW, Miller GG, Moore RB, Tulip J and McPhee MS. Hypocrellins as photosensitizers for photodynamic therapy: a screening evaluation and pharmacokinetic study. *Cancer Chemother. Pharmacol*., **37:** 343-350, 1996.
16. Yarosh DB. Liposomes in investigative dermatology (review). *Photodermatol. Photoimmunol. Photomed.*, **17**: 203-212, 2001.
17. Knuchel R, Hofstadter F, Jenkins WEA and Masters JRW. Sensitivities of monolayers and spheroids of the human bladder cancer cell line MGH-U1 to the drugs used for intravesical chemotherapy. *Cancer Res*., **49**: 1397-1401, 1989.
18. Erlichman C and Vidgen D. Cytotoxicity of adriamycin in MGH-U1 cells grown as monolayer cultures, spheroids, and xenografts in immune-deprived mice. *Cancer Res*., **44**: 5369-5375, 1984.
19. Sasaki T, Yamamoto M, Yamaguchi T. and Sugiyama S. Development of multicellular spheroids of Hela cells cocultured with fibroblasts and their response to X-irradiation. *Cancer Res*., **44**: 345, 1984.
20. Allen TM and Hansen CB. Pharmacokinetics of stealth versus conventional liposomes: effect of dose. *Biochim. Biophys. Acta*., **1068**: 133-141, 1991.

21. Stewart J. *Calculus*. 2nd Edition. Brooks/Cole Publishing Co. Pacific Grove, CA. 1991.
22. Boyle R and Dolphin D. Structure and biodistribution relationships of photodynamic sensitizers (review). *Photochem. Photobiol*., **64**: 469-485, 1996.
23. Diwu Z. Novel therapeutic and diagnostic applications of hypocrellins and hypericins. *Photochem. Photobiol*., **61**: 529-539, 1995.
24. Miller GG, Brown K, Ballangrud AM, Barajas O, Xiao Z, Tulip J, Lown JW, Leithoff JM, Allalunis-Turner MJ, Mehta R.D. and Moore R.B. Preclinical Assessment of Hypocrellin B and Hypocrellin B Derivatives as Sensitizers for Photodynamic Therapy of Cancer: Progress Update. *Photochem. Photobiol*., **65 (4)**: 714-722, 1997.
25. Xiao Z, Tamimi Y, Brown K, Tulip J and Moore RB. Interstitial photodynamic therapy in subcutaneously implanted urologic tumors in rats after intravenous administration of 5-aminolevulinic acid. *Urol. Oncol*., **7** (3): 125-132, 2002.
26. Waidelich R, Stepp H., Baumgartner R, Weninger E, Hofstetter A and Kriegmair M. Clinical experience with 5-aminolevulinic acid and photodynamic therapy for refractory superficial bladder cancer. *J. Urol*., **165**: 1904-1907, 2001.
27. Fukuda H, Casas A and Batlle A. Aminolevulinic acid: from its unique biological function to its star role in photodynamic therapy. Int. J. Biochem. Cell Biol., **37**(2):272-276, 2005.
28. Huygens A, Huyghe D, Bormans G, Verbruggen A, Kamuhabwa AR, Roskams T. and de Witte PAM. Accumulation and photocytotoxicity of hypericin and analogs in two- and three-dimensional cultures of transitional cell carcinoma cells. *Photochem. and Photobiol*., **78**(6): 607–614, 2003.
29. Glimelius B, Norling B, Nederman T and Carlsson J. Extracellular matrices in multicellular spheroids of human glioma origin: increased incorporation of proteoglycans and fiberonectin as compared to monolayer cultures. *Acta Pathol. Microbiol. Scand*. **96**: 433-444, 1988.
30. West CML. Size-dependent resistance of human tumor spheroids to photodynamic treatment. *Br. J. Cancer* **59**: 510-514, 1989.
31. Aveline BM, Hasan T and Redmond RW. The effects of aggregation on the photophysical properties of benzoporphyrin derivative-monoacid ring A (BPD-MA). *J. Photochem. Photobiol. B: Biol.*, **30**: 161-166, 1995.
32. Miller GG and Lown JW. Immunophotodynamic therapy: current developments and future prospects (review). *Drug Develop. Res.*, **42**: 182-197, 1997.
33. Kamuhabwa AA, Huygen A, de Witte PA. Photodynamic therapy of transitional cell carcinoma multicellular tumor spheroids with hypericin. *Int. J. Oncol*. 23:1445-1450, 2003.
34. Wang ZJ, He YY, Huang CG, Huang JS, Huang YC, An JY, Gu Y and Jiang LJ. Pharmacokinetics, tissue distribution and photodynamic therapy efficacy of liposomal-delivered hypocrellin A, a potential photosensitizer for tumor therapy. *Photochem. Photobiol*., **70**: 773-780, 1999.